Rotational spectrum and structure of the OCS–(CO$_2$)$_2$ trimer

Sean A. Peebles and Robert L. Kuczkowski[a)]

Department of Chemistry, The University of Michigan, Ann Arbor, Michigan 48109-1055

The rotational spectra of nine isotopes of the mixed trimer, OCS–(CO$_2$)$_2$, have been assigned using pulsed nozzle FTMW spectroscopy techniques. The structure resembles a distorted triangular cylinder. It can be thought of as the slipped (CO$_2$)$_2$ dimer with the OCS above the dimer and crossed about 23° to the axis of each CO$_2$. The distance between the carbon atoms on the CO$_2$ is 3.68(5) Å. The distance between the carbon on each CO$_2$ and the carbon on the OCS is 3.59(5) and 3.66(5) Å, respectively. The axes of the linear molecules are tilted 30°–35° from perpendicular relative to the edges of the C–C–C plane. The dipole moment components for the trimer are μ_a =0.63(2) D, μ_b=0.16(10) D and μ_c=0.21(2) D. The structure and dipole moment components are consistent with an interaction model, which includes a distributed multipole moment electrostatic analysis and atom–atom terms describing dispersion and repulsion. The structure is compared to other related dimers and trimers containing CO$_2$, OCS, and N$_2$O. © *1998 American Institute of Physics.* [S0021-9606(98)01937-0]

I. INTRODUCTION

High resolution spectroscopy investigations of trimer systems have been reported more frequently in recent years. Many of these trimers have been detected and assigned in searches for related dimers. Nevertheless, the number of trimers assigned is still small in comparison to the dimers investigated. As dimers are better understood and structural patterns delineated, it is attractive to systematically extend studies to related trimer systems. One expects trimers to exhibit van der Waals interactions and structures that resemble the associated dimers. This has been found in many cases, although differences in distances, or angles, or both are often found. These differences provide important insights on the balance of competitive interaction forces and changes due to the additional intermolecular interactions. Understanding these interactions should be helpful in modeling other trimers and larger systems.

Various dimers and trimers containing CO$_2$ and OCS have been studied in some detail in recent years, both by microwave and IR techniques. The CO$_2$–OCS dimer[1] and the CO$_2$ dimer[2] have both been characterized and their planar, slipped parallel type structures are well known. The nonpolar OCS dimer has likewise been identified,[3] although the polar form of this species still awaits a study by high resolution techniques, despite evidence for its existence in MBER experiments.[4] Two forms of the CO$_2$ trimer have been studied using IR techniques. Both a planar cyclic[5] and noncyclic cylinderlike structure[6] have been identified. Recently, a study of the cylinderlike OCS trimer was reported,[7] which prompted us to ask whether a mixed trimer of OCS and CO$_2$ could be found. Since a sample mixture containing OCS and CO$_2$ can give rise to only two possible mixed trimers (if we exclude any possible associations that also include a rare gas atom) and since all of the monomers are

relatively simple linear triatomics, an attempt was made to identify and characterize one of these systems. Mixed trimer systems containing the CO$_2$ dimer (CO$_2$–CO$_2$–H$_2$O[8,9] and CO$_2$–CO$_2$–HCN[10]) have already been studied by microwave techniques.

II. EXPERIMENT

The rotational spectrum of the CO$_2$–CO$_2$–OCS trimer was observed using a Balle–Flygare-type Fourier transform microwave spectrometer[11] with a pulsed supersonic nozzle source. Initial searches were carried out on the University of Michigan spectrometer,[12] which was recently upgraded to an autoscan mode using software and hardware developments at the University of Kiel.[13] The searches were conducted over a 2 GHz region between 6 and 8 GHz in order to locate likely transitions, using known (OCS)$_3$[7] and CO$_2$–CO$_2$–H$_2$O[8] transitions as a guide for optimum valve conditions and sample quality. After mixing tests and the elimination of all known dimer and trimer transitions in the search region (including numerous OCS trimer transitions), Stark effect measurements were carried out on four of the strongest remaining lines to attempt to deduce their J values. Successful assignments of these four lines based on their Stark effects led to the measurement of a total of 52 transitions for the normal species. Stark effect measurements were conducted by the application of voltages up to ±9 kV to a pair of parallel 50 cm×50 cm steel mesh plates that are separated by about 30 cm and situated inside the evacuated cavity. The electric field was calibrated on each day of measurement using the J=1←0 transition of OCS, assuming a dipole moment of 0.7152 D.[14] A number of lines found in the initial search region were unassigned after measurement of the rotational spectra of this species. We have recently assigned several of these lines to the other mixed trimer (OCS)$_2$CO$_2$.

The CO$_2$–CO$_2$–OCS trimer was generated in a supersonic expansion using a gas mixture composed of approxi-

[a)]Electronic mail: kuczkows@umich.edu

TABLE I. Observed rotational transitions (in MHz) for the normal isotopomer of CO_2–CO_2–OCS.

$J'_{K_a K_c}$	$J''_{K_a K_c}$	ν_{obs}/MHz	$\Delta\nu$/kHz[a]
4_{14}	3_{13}	5632.9738	0.3
4_{04}	3_{03}	5669.3350	1.1
3_{22}	2_{11}	5843.1823	1.7
3_{12}	2_{02}	6351.3522	4.3
4_{23}	3_{22}	6365.5590	5.3
3_{21}	2_{11}	6460.1737	−3.4
4_{13}	3_{12}	6687.0935	−0.7
4_{32}	3_{31}	6695.3536	0.6
3_{22}	2_{12}	6818.3686	0.8
5_{05}	4_{14}	6939.0590	1.7
4_{31}	3_{30}	6941.3369	−5.3
5_{15}	4_{14}	6942.3302	−0.2
5_{05}	4_{04}	6952.5397	0.1
5_{15}	4_{04}	6955.8098	−3.0
4_{23}	3_{12}	6983.6661	−1.7
4_{22}	3_{21}	7172.0914	−0.3
3_{31}	2_{20}	7235.6710	0.8
3_{30}	2_{20}	7285.3384	3.8
3_{31}	2_{21}	7386.4436	5.5
3_{21}	2_{12}	7435.3650	0.6
3_{30}	2_{21}	7436.1056	3.2
3_{21}	2_{02}	7586.4558	−2.8
5_{14}	4_{23}	7674.1511	−6.3
5_{24}	4_{23}	7782.8348	−1.4
5_{14}	4_{13}	7970.7319	0.9
6_{06}	5_{15}	8241.9710	−3.1
6_{16}	5_{15}	8242.7142	−3.5
6_{06}	5_{05}	8245.2530	5.8
6_{16}	5_{05}	8245.9927	1.8
5_{33}	4_{32}	8312.4562	−1.2
4_{22}	3_{12}	8407.1978	−4.6
5_{42}	4_{41}	8439.4471	5.2
5_{41}	4_{40}	8534.2089	0.8
4_{32}	3_{21}	8597.7802	0.0
4_{13}	3_{03}	8637.5982	−0.5
4_{23}	3_{13}	8884.3271	−2.5
4_{31}	3_{21}	8893.4310	−2.8
5_{32}	4_{31}	8905.8263	5.5
6_{15}	5_{24}	9103.7365	−6.0
6_{25}	5_{24}	9136.8728	2.2
6_{15}	5_{14}	9212.4241	2.8
4_{32}	3_{22}	9214.7782	1.4
6_{34}	5_{33}	9842.8673	0.7
4_{41}	3_{30}	9898.4118	−0.7
4_{40}	3_{30}	9911.8272	−0.7
4_{41}	3_{31}	9948.0747	−2.2
4_{40}	3_{31}	9961.4886	−3.6
6_{43}	5_{42}	10 145.7272	−0.9
5_{23}	4_{13}	10 567.0121	−7.0
6_{33}	5_{32}	10 793.3288	1.5
5_{14}	4_{04}	10 939.0019	6.1
5_{24}	4_{14}	11 034.1943	2.1

[a]$\Delta\nu = \nu_{obs} - \nu_{calc}$.

mately 1.5% CO_2 and 1.5% OCS seeded in 97% He–Ne "first run" mixture (80% Ne, 20% He). The backing pressure of the carrier was about 3 atm. Experiments with Ar as the carrier gas resulted in a significant reduction in the intensity of the transitions, probably due to complexation of the monomers with the more polarizable Ar. The He/Ne/OCS/CO_2 mixture was expanded into the evacuated Fabry–Perot cavity through a modified Bosch fuel injector valve,

perpendicular to the direction of microwave propagation. C $^{18}O_2$ (97.55% ^{18}O, Icon) was used to observe the C $^{18}O_2$ isotopes, either as part of a 1:1 mixture with OCS for the (C $^{18}O_2)_2$–OCS species or mixed in the ratio 1:3:4 with normal C $^{16}O_2$ and OCS in order to form singly substituted (C ^{16}O ^{18}O)–(C ^{16}O ^{16}O)–OCS isotopomers. Instead the doubly substituted (C $^{16}O_2$)–(C $^{18}O_2$)–OCS isotopomers were found. Apparently, ^{18}O–^{16}O random scrambling was modest, unlike in a previous study in our lab.[15] ^{18}OCS (93.4% ^{18}O), O ^{13}CS (99% ^{13}C), and $^{13}CO_2$ (99% ^{13}C) were purchased from Isotec to observe the remaining isotopomers. A 1:1 mixture of $^{12}CO_2$ and $^{13}CO_2$ was combined in the sample bulb with OCS to find the two singly substituted $^{12}CO_2$–$^{13}CO_2$–OCS isotopomers.

Linewidths were about 30 kHz full width at half-maximum. The transition frequencies were reproducible to 2 kHz for strong lines with a resolution element of 4 kHz. The strongest four transitions (at 6365.559, 6687.094, 6942.330, and 6952.540 MHz) were readily observed in an autoscan mode with 300 gas pulses. Some of the weaker isotopic species required typically 6000 shots for reliable frequency measurements. No evidence of splitting in the transitions was seen under these somewhat "low resolution" conditions.

III. RESULTS AND ANALYSIS

A. Spectra

a-, *b*-, and *c*-type transitions were observed for all isotopic species, with the *a*-type lines by far the most intense and the *b*-type lines the weakest. The measured frequencies of 52 transitions for the normal species of CO_2–CO_2–OCS are given in Table I, along with the residuals from a fit of these lines to a Watson A-reduction Hamiltonian in the I^r representation. The fitted rotational and centrifugal distortion constants for this and the other isotopic species are given in Tables II–IV. The value of Δ_K was held fixed at zero in all fits since its inclusion led to a poorly determined value and had no significant effect on the fitted constants. The standard Watson Hamiltonian was clearly sufficient for a good fit of the measured transitions. The spectra of the following isotopic species were also observed: $(CO_2)_2O$ ^{13}CS, $(CO_2)_2$ ^{18}OCS, $(^{13}CO_2)_2$OCS, $(^{12}CO_2)(^{13}CO_2)$OCS, $(^{13}CO_2)(^{12}CO_2)$OCS, (C $^{18}O_2)_2$OCS, (C $^{18}O_2)$(C $^{16}O_2)$OCS, and (C $^{16}O_2)$(C $^{18}O_2)$OCS. Transition frequencies for all the isotopic species are available as supplementary material.[16]

B. Dipole moment

Six rotational transitions (a total of 13 components in all) yielded useful dipole moment data from their Stark effects. The observed Stark coefficients and computed dipole components are listed in Table V. The dipole components in Table V are those that result from the least squares fit of all the *M* components given in the table. Experimentation with the deletion of various components in the fits underscored the need for generous error estimates. This was especially apparent for the μ_b component. The poor determination of this component is due mainly to the very small contribution it makes to the measured frequency shifts. Also, transitions with complications from near *a*- and *c*-dipole degeneracies

TABLE II. Spectroscopic constants for the normal and OCS enriched isotopomers.

Spectroscopic constant	CO_2–CO_2–OCS	CO_2–CO_2–O^{13}CS	CO_2–CO_2–^{18}OCS
A/MHz	1299.1360(4)	1290.8732(4)	1270.8277(4)
B/MHz	973.7407(3)	972.1569(3)	972.0142(3)
C/MHz	648.6624(3)	646.0122(3)	642.2204(3)
Δ_J/kHz	1.270(5)	1.261(5)	1.247(6)
Δ_{JK}/kHz	2.41(2)	2.35(2)	2.19(2)
δ_J/kHz	0.336(2)	0.332(2)	0.334(3)
δ_K/kHz	1.95(1)	1.91(1)	1.85(1)
$\Delta\nu_{rms}$/kHz[a]	3.19	3.12	3.32
N[b]	52	45	43

[a]$\Delta\nu_{rms} = [\Sigma(\nu_{obs} - \nu_{calc})^2/N]^{1/2}$.
[b]N is the number of fitted transitions.

were avoided; the observed shifts were at least three orders of magnitude smaller than the smallest energy differences in the calculated perturbation sums. Consequently, we recommend the following dipole moments for this complex: $\mu_a = 0.63(2)$ D, $\mu_b = 0.16(10)$ D, and $\mu_c = 0.21(2)$ D. The closeness of the total dipole moment $[\mu_{tot} = 0.69(5)$ D$]$ to that of the OCS monomer (0.7152 D[14]) was a useful early indication of the nature of the species that we had assigned (i.e., a trimer that probably contains just a single OCS molecule).

C. Structure

The eight isotopomers and the normal species allow us to locate the atoms of this trimer reasonably well. Single isotopic substitution at the O and C atoms in the OCS molecule and at the carbon atoms of the CO_2 enabled a Kraitchman substitution determination[17] of these atom positions. This located the three carbon atoms and the OCS molecule as a whole in the principal axis system (although there was, for a while, an ambiguity in the sign of one of the carbon atoms of the CO_2). This results in a substitution structure value for the three (C··C) distances that are given in Table VII.

Efforts to determine the orientation of the CO_2 molecules proved to be more difficult. Initially we tried to locate the oxygen atoms using the University of Michigan STRFIT87 and STRFITQ implementations of Schwendeman's original STRFIT programs.[18] The former program fits the principal axes Cartesian coordinates of the atoms to the observed mo-

ments of inertia, while the latter fits internal coordinates (Thompson distances and angles[19]). The bond distances and angles of OCS and CO_2 were held fixed at the monomer values (cf. below) in the fitting. Although sufficient fitting equations seemed to be in hand, the least square fits of the inertial data failed to converge when using the normal species, $(CO_2)_2$ ^{13}CS, $(CO_2)_2$ ^{18}OCS, $(^{13}CO_2)(^{12}CO_2)$OCS, $(^{12}CO_2)(^{13}CO_2)$OCS, and $(C$ $^{18}O_2)_2$OCS data. It was evident that an asymmetric ^{18}O carbon dioxide species was needed to break linear dependencies in the fitting equations. A search for additional ^{18}O labeled CO_2 species was then initiated to better locate the oxygen atoms. The two doubly substituted species $(C$ $^{18}O_2)(C$ $^{16}O_2)$OCS were identified (cf. Sec. II), and this proved sufficient to obtain a unique structure by least square fitting of the 27 moments of inertia using the STRFITQ algorithm.

Nine parameters are needed to define the structure of the trimer. The parameters actually fitted were the distances C_1–M_3 and C_2–M_3 between the carbons on each CO_2 and M_3 (center of mass) of the OCS, and angle (C_1–M_3–C_2) fixing the center of masses of the monomers. In addition, three planar angles formed by the axis of each linear molecule with the C_1–C_2, C_1–M_3, and C_2–M_3 axes were determined and three dihedral angles viewed down the C_1–C_2, C_1–M_3, and C_2–M_3 axes. These quantities and other derived parameters of interest are given in Table VII. Many additional parameters are illustrated in Figs. 1–4.

The deviation of the fit $[\Delta I_{rms} = 0.25$ amu Å^2, where $\Delta I = I_x(calc) - I_x(obs)]$ was reasonably small and could be

TABLE III. Spectroscopic constants for the ^{13}C doubly and singly substituted CO_2 isotopomers.

Spectroscopic constant	$^{13}CO_2$–$^{13}CO_2$–OCS	$^{12}CO_2$–$^{13}CO_2$–OCS	$^{13}CO_2$–$^{12}CO_2$–OCS
A/MHz	1284.2737(5)	1284.9998(8)	1298.3852(7)
B/MHz	962.5747(3)	973.0110(7)	963.3368(7)
C/MHz	640.5321(4)	644.9967(5)	644.1642(5)
Δ_J/kHz	1.251(6)	1.32(1)	1.27(1)
Δ_{JK}/kHz	2.38(2)	2.11(6)	2.27(5)
δ_J/kHz	0.327(2)	0.361(7)	0.336(6)
δ_K/kHz	1.94(2)	2.07(3)	2.03(3)
$\Delta\nu_{rms}$/kHz[a]	3.55	3.22	3.16
N[b]	44	23	24

[a]$\Delta\nu_{rms} = [\Sigma(\nu_{obs} - \nu_{calc})^2/N]^{1/2}$.
[b]N is the number of fitted transitions.

TABLE IV. Spectroscopic constants for the [18]O labeled CO_2 isotopomers.

Spectroscopic constant	$C^{18}O_2-C^{18}O_2-OCS$	$C^{16}O_2-C^{18}O_2-OCS$	$C^{18}O_2-C^{16}O_2-OCS$
A/MHz	1225.1019(5)	1236.1185(10)	1286.7473(10)
B/MHz	915.3689(3)	963.0407(7)	925.8453(6)
C/MHz	613.9393(4)	632.3685(4)	629.5346(5)
Δ_J/kHz	1.141(6)	1.22(1)	1.181(9)
Δ_{JK}/kHz	2.21(2)	2.39(4)	2.16(4)
δ_J/kHz	0.289(3)	0.317(6)	0.310(5)
δ_K/kHz	1.71(2)	1.95(3)	1.67(3)
$\Delta\nu_{rms}$/kHz[a]	3.20	2.66	3.03
N[b]	36	21	20

[a]$\Delta\nu_{rms} = [\Sigma(\nu_{obs}-\nu_{calc})^2/N]^{1/2}$.
[b]N is the number of fitted transitions.

further reduced by deleting the $(C^{18}O_2)_2OCS$ data. Dropping this isotopomer from the fit improved the deviation significantly ($\Delta I_{rms}=0.17$ amu Å^2). Since weakly bound complexes often exhibit large-amplitude motions of their monomer subunits, the measured rotational constants contain contamination from these vibrations. The effect of these motions is likely to be greatest in the $(C^{18}O_2)_2OCS$ species and responsible for the larger deviation when it is included. During the fitting, the monomer geometries were held fixed at the literature values $[r(C-O)=1.162$ Å in CO_2;[20] $r(C-O)=1.1561$ Å and $r(C-S)=1.5651$ Å in OCS[21]], a common assumption in the fitting of weakly bound dimer structures. Indeed, the calculated O—C bond length in OCS from the Kraitchman substitution coordinates is 1.1637 Å, an increase of less than 0.008 Å from the literature value. The Cartesian coordinates in the principal axis frame that result from the inertial fit are given in Table VI. Table VI also includes the principal axis substitution coordinates for the O and C atoms of OCS and the C atoms of the CO_2 derived from the Kraitchman single substitution calculations. These are in reasonable agreement with those from the fit of the moments of inertia. Table VII lists some of the structural

parameters that result from the coordinates in Table VI as well as the values derived from the substitution structure and from a theoretical model to be discussed later.

The structural parameters from the inertial fit are r_0 values, that is, parameters obtained by fitting ground state moments of inertia, ignoring any vibrational contributions to them. Uncertainties in these parameters are given in Table VII; these are the statistical uncertainties from the fitting process and do not contain any model errors from the neglect of vibrations. These model errors can be larger than the statistical values in weakly bond complexes. It is not easy to estimate them without some information on the vibrations. Nevertheless, there are several indicators that the derived parameters are reasonable estimates of the structural details: the consistency of the fit, the small distortion constants, the consistency checks between the r_0 parameters, the Kraitchman values and the monomer bond distances, and the absence of tunneling splittings. We would expect that the equilibrium parameters would fall within ±0.05 Å and ±5° of the values in the tables and figures.

IV. DISCUSSION

A. Empirical considerations

It is apparent in Fig. 2(b) that the trimer has the rough shape of a cylinder (or barrel), although the acute angles that

TABLE V. Stark coefficients and dipole moments for CO_2-CO_2-OCS.

Transition	$\|M\|$	$\Delta\nu/\epsilon^{2}$[a]	Obs.−Calc.
$4_{13}-3_{12}$	1	−0.088	−0.011
	2	−0.229	−0.025
	3	−0.452	−0.036
$4_{23}-3_{22}$	2	1.460	0.078
	3	2.929	−0.144
$3_{12}-2_{02}$	1	0.892	0.118
$3_{21}-2_{02}$	1	1.287	0.188
	2	4.916	−0.119
$3_{22}-2_{12}$	1	−0.940	−0.110
	2	−2.921	−0.024
$4_{22}-3_{21}$	1	−0.355	−0.061
	2	−1.416	−0.195
	3	−2.836	−0.071
	$\mu_a=0.63(2)$ D[b]		
	$\mu_b=0.16(10)$ D[b]		
	$\mu_c=0.21(2)$ D[b]		

[a]Observed Stark coefficients in units of 10^{-5} MHz/(V cm$^{-1})^2$.
[b]Uncertainties result from fitting of all the listed transitions. Variation of the set of fitted transitions results in a deviation in the values which the uncertainty range accommodates—see the text for a full discussion.
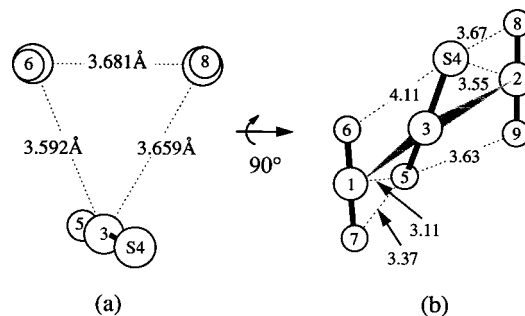

FIG. 1. Interatomic distances in the CO_2-CO_2-OCS trimer. Note that the perspective in (a) places the carbon of OCS in the plane of the paper, the carbon of the left CO_2 somewhat above the plane, and the carbon of the right CO_2 somewhat below the plane. The perspective in (b) is obtained by rotating (a) by 90° about the arrow in the plane of the paper. In perspective (b), the two CO_2 monomers are almost coplanar: $\tau(7\text{-}1\text{-}2\text{-}9)=-7.7°$. All distances are given in Å.
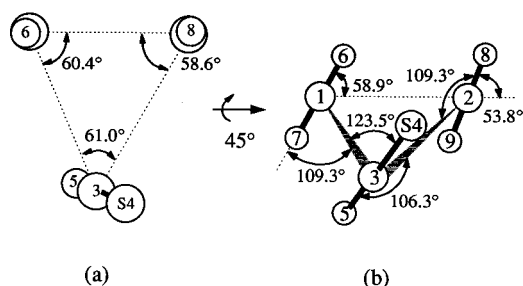
FIG. 2. Planar angles in the CO_2–CO_2–OCS trimer. The perspective (a) is the same as Fig. 1(a). (b) is obtained by rotating (a) about 45° about the arrow to better illustrate the angles between the triatomic axes and the ring C–C axes. Dihedral angles around the ring: $\tau(7\text{-}1\text{-}2\text{-}9)=-7.7°$, $\tau(7\text{-}1\text{-}3\text{-}5)=-23.0°$, $\tau(9\text{-}2\text{-}3\text{-}5)=-23.5°$. Distances are in Å.

the linear axes make relative to the C–C–C plane ($\sim50°$–70°) suggest a better description may be a tilted, somewhat triangular cylinder. Of course, the faces of the cylinder are not actually flat since the dihedral angles along the C–C axes deviate from 0° or 180°.

The three monomers orient themselves to resemble the constituent dimer structures to a great extent with the notable change that the OCS crosses the CO_2 axes to better interact with each CO_2. This is illustrated in Figs. 3 and 4. Figure 3 reveals that the CO_2–CO_2 face in the trimer is slightly expanded and less symmetric than the CO_2 dimer. The two CO_2's are nearly coplanar, deviating 7° from coplanarity. The crossing of the OCS to each CO_2 axis is more noticeable; the deviation in coplanarity of the OCS and each CO_2 is about 22°. Still one CO_2–OCS face [Fig. 4(c)] closely resembles the CO_2–OCS dimer in interatomic distances and planar angles to the C–C axes. The second CO_2–OCS face [Fig. 4(b)] is markedly different from the dimer. This CO_2 has slipped so that the top oxygen (O_6) and carbon (C_1) in the CO_2 are close to the carbon (C_3) and oxygen (O_5) in the OCS. The O_6–C_3 distance of 3.39 Å and the O_5–C_1 distance of 3.11 Å are among the shortest nonbonded approaches in the trimer and compare to the value of 3.15 Å in the CO_2 dimer. It is noteworthy that these presumably favorable interactions also bring O_5 and O_7 within 3.37 Å. In summary, the trimer can be described as a CO_2 dimer slightly perturbed by an OCS addend lying above the dimer.

In contrast, it is interesting that the CO_2 dimer moiety found in $(CO_2)_2$–H_2O[9] and $(CO_2)_2$–HCN[10] are more per-

turbed with the C–C distance shortening to about 3.50–3.52 Å, forcing the CO_2's to deviate about 20° from planarity.

The $(CO_2)_2$OCS trimer closely resembles the noncyclic CO_2 trimer.[6] The structure of this latter trimer was cleverly deduced from vibrational transition dipole data and rotational constants. It has a barrel-like structure with one CO_2 tilted relative to a CO_2 dimer fragment similar to the OCS in $(CO_2)_2$OCS. The dihedral angles between the tilted CO_2 and the CO_2's in the dimer fragment are approximately 27(7)°. The CO_2 dimerlike fragment is nearly coplanar [$\tau = 5.8(4)°$]. Its C–C distance is 3.76(8) Å and these carbons are 3.55(5) Å from the crossed CO_2.

The barrel-like $(OCS)_3$[7] and $(NNO)_3$[23] structures recently proposed also resemble the $(CO_2)_2$OCS trimer. The N_2O trimer appears to have a less planar N_2O dimer fragment and the third N_2O is more crossed relative to the dimer fragment. The structure for $(OCS)_3$ is less precisely known at

FIG. 4. A comparison of the CO_2–OCS dimer (a) with the CO_2–OCS faces (b), (c) of the $(CO_2)_2$OCS trimer. Distances are in Å.
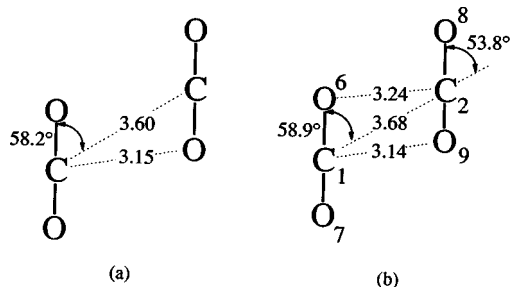

FIG. 3. A comparison of the CO_2 dimer (a) and the CO_2 dimer face of the $(CO_2)_2$OCS trimer (b). Distances are in Å.

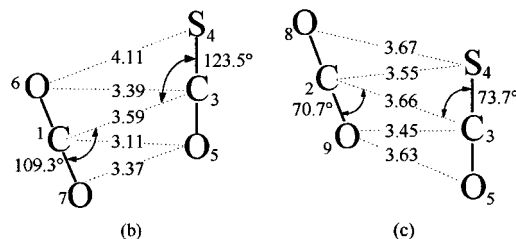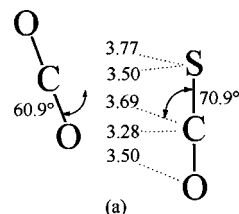TABLE VI. Principal axis coordinates determined from a least squares fit of the inertial data (Å). Absolute values in brackets for the carbons of CO_2 and the C and O atoms of OCS are the Kraitchman substitution coordinates obtained from the single isotopic substitution data.

Atom[a]	a	b	c
C_1	2.323 78	0.212 89	0.464 74
	|2.329 13|	|0.176 74|	|0.445 47|
C_2	−0.449 18	−2.057 72	−0.374 73
	|0.510 85|	|2.04 44|	|0.350 87|
C_3	−0.927 58	1.567 56	−0.240 79
	|0.874 01|	|1.562 85|	|0.265 91|
M_3	−1.375 16	1.353 30	−0.066 03
S_4	−2.259 10	0.930 16	0.279 11
O_5	0.055 98	2.038 39	−0.624 82
	|0.130 51|	|1.980 34|	|0.679 32|
O_6	1.574 53	−0.146 21	1.277 08
O_7	3.073 03	0.571 99	−0.347 61
O_8	−1.169 75	−2.568 71	0.380 19
O_9	0.271 40	−1.546 73	−1.129 65

[a]See Fig. 1 for the atom numbers. M_3 is the center of mass of the OCS.

TABLE VII. A comparison of structural parameters determined for the CO_2–CO_2–OCS trimer. See Fig. 1 for atom numbering.[a]

Parameter	Inertial fit	Kraitchman (r_s)	Model
$r(C_1—C_2)$/Å	3.681(16)	3.692	3.75
$r(C_2—C_3)$/Å	3.659(16)	3.627	3.61
$r(C_1—C_3)$/Å	3.592(14)	3.562	3.57
$r(C_1—M_3)$/Å	3.907(11)	⋯	3.89
$r(C_2—M_3)$/Å	3.548(12)	⋯	3.48
$\angle(C_1—M_3—C_2)$/°	58.9(2)	⋯	60.8
$\angle(O_8—C_2—M_3)$/°	101.8(35)	⋯	111.6
$\angle(O_7—C_1—C_2)$/°	121.1(21)	⋯	126.3
$\angle(S_4—M_3—C_1)$/°	129.9(10)	⋯	130.3
$\tau(O_8—C_2—M_3—C_1)$/°	124.6(17)	⋯	123.5
$\tau(O_7—C_1—C_2—M_3)$/°	−100.9(34)	⋯	−111.1
$\tau(S_4—M_3—C_1—C_2)$/°	44.2(18)	⋯	40.9

[a]Signs in the dihedral angles are consistent with the definition in Ref. 22. The last nine parameters in the table were quantities determined by least squares fitting of the 27 moments of inertia. The first three parameters were derived from this fit (column 2) or from Kraitchman's single substitution equations (Ref. 17) (column 3), which uses only six moments of inertia for each quantity. See the text for a description of model parameters (column 4).

TABLE VIII. A comparison of experimental and predicted constants for CO_2–CO_2–OCS.

Constant	Experimental	Predicted[a]
A/MHz	1299.1360(4)	1346
B/MHz	973.7407(3)	977
C/MHz	648.6624(3)	646
μ_a/D	0.63(2)	0.67
μ_b/D	0.16(10)	0.25
μ_c/D	0.21(2)	0.23

[a]The predicted rotational constants were obtained from the ORIENT program (see the text). The predicted dipole was obtained from a projection of the OCS monomer dipole of the model structure (recovered from the distributed multipole moments for that molecule) into the principal axis system.

this time and a comparison of parameters is therefore less useful.

In summary, it is apparent that this distorted cylinderlike motif is endemic to three homomolecular trimers of CO_2, NNO, and OCS and the mixed trimer of $(CO_2)_2$OCS reported in this paper. Of course, the possibility of identifying other isomeric forms is still an open question and, in fact, the CO_2 cyclic planar (pinwheel) structure was the first trimer species identified in this set. The cylindrical form is one that allows maximum contact optimizing the dispersion forces while the slipping and tilting of the monomers maximizes the electrostatic attraction.

B. Theoretical modeling

After initial assignment of the normal species, we explored a theoretical model to predict the structure. We were interested in checking whether the model would provide rotational constants that might confirm our postulated carrier of the spectrum and assist us in the location of further isotopic species. The model employed included a distributed multipole electrostatic interaction and an analytical dispersion and repulsion term. The ORIENT program of Stone[24] was employed for the calculations. One energy minimum on the potential energy surface of the trimer was found, starting with a planar cyclic pinwheel configuration. The distributed multipole moments were calculated for the CO_2 and OCS molecules at the SCF level with the CADPAC suite of programs[25] using a TZ2P basis set, and these provided the electrostatic contribution to the intermolecular interaction potential. Moments up to the hexadecapole terms were used and are available as supplementary material.[16] The dispersion and repulsion energies were included as atom–atom terms. The combined dispersion and repulsion energy between two molecules A and B were represented by[26]

$$U_{\text{exp}-6} = \sum_{i,j} K \exp[-\alpha_{ij}(R_{ij}-\rho_{ij})] - \frac{C_6^{ij}}{R_{ij}^6}, \qquad (1)$$

where i and j represent sites on molecules A and B, respectively, separated by a distance R_{ij}. α_{ij} is a hardness parameter and is dependent upon a particular site pair. The parameter ρ_{ij} is orientation dependent and describes the effective size of the atoms. K is simply a convenient unit of energy and has been taken to be $10^{-3}E_h$ in the present work. Values of α_{ij}, ρ_{ij}, and C_6^{ij} were taken from the tabulated values of Mirsky[27] and were obtained from Table 11.2 of Ref. 26. Atom–atom terms for pairs of atoms that were not included in Ref. 26 were obtained by the following combination rules: the harmonic mean for α (i.e., $1/\alpha_{ij} \approx 1/\alpha_i + 1/\alpha_j$), the arithmetic mean for ρ, and the geometric mean for C_6. A noncyclic, barrel-like structure in which the three monomers are aligned almost parallel was predicted from this model, with an interaction energy of -1613.2 cm^{-1}. The computed rotational constants for this species were in remarkably close agreement with the measured constants (see Table VIII) and, taking into account the agreement in predicted dipole moment components, it is clear that this model is a good approximation of the actual structure. Isotopic substitution of the atoms in this model structure led to a quick identification of the isotopic species' spectra, further indicating that this predicted structure was an excellent working model to the actual structure. The computed distances for the C··C separations in the model are 3.60 Å (CO_2–OCS) and 3.75 Å (CO_2–CO_2). The fitted values are 3.592 and 3.659 Å for the former and 3.681 Å for the latter. While the details are somewhat less than perfect, the agreement is quite good and certainly helpful in a spectroscopic sense (Table VIII). This indicates that the physics of the interaction and the resultant structure can be largely accommodated by the electrostatic–dispersion–repulsion mechanism. The usefulness of the ORIENT model was gratifying, although we note that it has proved somewhat less successful in reproducing the structural/spectral features for several SO_2 containing dimers,[28] which we have investigated. It will be worthwhile to learn if it is similarly successful in applications to other dimers and trimers containing linear molecules, and we intend to explore this in subsequent studies. Similar models patterned after Muenter's formalism and that of others have been previously employed in an analysis of the CO_2 dimers[29] and trimers[6,30] and the OCS trimer[7] with comparable success. The use of molecular dipole and quadrupole moment information has also been explored for the CO_2–OCS dimer[1] and the cyclic CO_2 trimer,[5] where the simplicity of the structural

systems made this approach attractive. This approach is less useful for this case. It is apparent that while the basic tilted barrel shape of the $(CO_2)_2OCS$ trimer can be qualitatively rationalized as an optimal compromise between dispersion forces seeking close contact (three parallel sticks), and electrostatic forces driving the slipping and sliding of the sticks with repulsion keeping them apart, a more complex atom–atom interaction model such as afforded by the ORIENT program is needed to rationalize the details. Some induction interaction forces will likely also be needed to fine tune the details, although this contribution appears to be small, based on the small effect on the observed dipole moment. An optimal model to closely reproduce the physical system will probably also need to account for anisotropy in the interaction terms as well.

ACKNOWLEDGMENTS

[1] S. E. Novick, R. D. Suenram, and F. J. Lovas, J. Chem. Phys. **88**, 687 (1988).

[2] M. A. Walsh, T. H. England, T. R. Dyke, and B. J. Howard, Chem. Phys. Lett. **142**, 265 (1987); K. W. Jucks, Z. S. Huang, R. E. Miller, G. T. Fraser, A. S. Pine, and W. J. Lafferty, J. Chem. Phys. **88**, 2185 (1988).

[3] R. W. Randall, J. M. Wilkie, B. J. Howard, and J. S. Muenter, Mol. Phys. **69**, 839 (1990).

[4] J. M. LoBue, J. K. Rice, and S. E. Novick, Chem. Phys. Lett. **112**, 376 (1984).

[5] G. T. Fraser, A. S. Pine, W. J. Lafferty, and R. E. Miller, J. Chem. Phys. **87**, 1502 (1987).

[6] M. J. Weida and D. J. Nesbitt, J. Chem. Phys. **105**, 10 210 (1996).

[7] J. P. Connelly, A. Bauder, A. Chisholm, and B. J. Howard, Mol. Phys. **88**, 915 (1996).

[8] K. I. Peterson, R. D. Suenram, and F. J. Lovas, J. Chem. Phys. **90**, 5964 (1989).

[9] H. S. Gutowsky and C. Chuang, J. Chem. Phys. **93**, 894 (1990).

[10] H. S. Gutowsky, J. Chen, P. J. Hajduk, and R. S. Ruoff, J. Phys. Chem. **94**, 7774 (1990).

[11] T. J. Balle and W. H. Flygare, Rev. Sci. Instrum. **52**, 33 (1981).

[12] K. W. Hillig, II, J. Matos, A. Scioly, and R. L. Kuczkowski, Chem. Phys. Lett. **133**, 359 (1987).

[13] J-U. Grabow, Ph.D. Thesis, University of Kiel, 1992.

[14] J. S. Muenter, J. Chem. Phys. **48**, 4544 (1968).

[15] L. Sun, I. I. Ioannou, and R. L. Kuczkowski, Mol. Phys. **88**, 255 (1996).

[16] See AIP Document No. E-PAPS: E-JCPSA6-109-019837 for tables of isotopic frequencies and distributed multipole moments. E-PAPS document files may be retrieved free of charge from our FTP server (http://www.aip.org/epaps/epaps.html) or from ftp.aip.org in the directory /epaps/. For further information: e-mail paps@aip.org or fax: 516-576-2223.

[17] J. Kraitchman, Am. J. Phys. **21**, 17 (1953).

[18] R. H. Schwendeman, in *Critical Evaluation of Chemical and Physical Structural Information*, edited by D. R. Lide and M. A. Paul, Washington DC, National Academy of Sciences, 1974.

[19] H. B. Thompson, J. Chem. Phys. **47**, 3407 (1967).

[20] E. K. Plyler, L. R. Blaine, and E. D. Tidwell, J. Res. Natl. Bur. Stand. **55**, 183 (1955).

[21] Y. Morino and C. Matsumura, Bull. Chem. Soc. Jpn. **40**, 1095 (1967); A. G. Maki and D. R. Johnson, J. Mol. Spectrosc. **47**, 226 (1973).

[22] E. B. Wilson, Jr., J. C. Decius, and P. C. Cross, *Molecular Vibrations* (McGraw-Hill, New York, 1955).

[23] R. E. Miller and L. Pedersen, J. Chem. Phys. **108**, 436 (1998).

[24] A. J. Stone, A. Dullweber, M. P. Hodges, P. L. A. Popelier, and D. J. Wales, ''ORIENT: A program for studying interactions between molecules, Version 3.2,'' University of Cambridge, 1995.

[25] CADPAC: The Cambridge Analytic Derivatives Package Issue 6, Cambridge, 1995. A suite of quantum chemistry programs developed by R. D. Amos with contributions from I. L. Alberts, J. S. Andrews, S. M. Colwell, N. C. Handy, D. Jayatilaka, P. J. Knowles, R. Kobayashi, K. E. Laidig, G. Laming, A. M. Lee, P. E. Maslen, C. W. Murray, J. E. Rice, E. D. Simandiras, A. J. Stone, M.-D. Su, and D. J. Tozer.

[26] A. J. Stone, *The Theory of Intermolecular Forces* (Clarendon, Oxford, 1996).

[27] K. Mirsky, ''The determination of the intermolecular interaction energy by empirical methods,'' in *Computing in Crystallography*, edited by R. Schenk, R. Olthof-Hazenkamp, H. van Koningveld and G. C. Bassi (Delft University Press, 1978).

[28] S. A. Peebles and R. L. Kuczkowski, J. Mol. Struct. **447**, 151 (1998).

[29] J. S. Muenter, J. Chem. Phys. **94**, 2781 (1991).

[30] M. J. Weida, J. M. Spherac, and D. J. Nesbitt, J. Chem. Phys. **103**, 7685 (1995).

[31] S. A. Peebles and R. L. Kuczkowski, Chem. Phys. Lett. **286**, 421 (1998).